AAS 15-545

COMPARISON OF NON-INTRUSIVE APPROACHES TO UNCERTAINTY PROPAGATION IN ORBITAL MECHANICS

Chiara Tardioli[*], Martin Kubicek[*], Massimiliano Vasile[†], Edmondo Minisci [‡], Annalisa Riccardi[§]

The paper presents four different non-intrusive approaches to the propagation of uncertainty in orbital dynamics with particular application to space debris orbit analysis. Intrusive approaches are generally understood as those methods that require a modification of the original problem by introducing a new algebra or by directly embedding high-order polynomial expansions of the uncertain quantities in the governing equations. Non-intrusive approaches are instead based on a polynomial representations built on sparse samples of the system response to the uncertain quantities. The paper will present a standard Polynomial Chaos Expansion, an Uncertain Quantification-High Dimensional Model Representation, a Generalised Kriging model and an expansion with Tchebycheff polynomials on sparse grids. The work will assess the computational cost and the suitability of these methods to propagate different type of orbits.

INTRODUCTION

Uncertainty propagation in orbital mechanics is a key enabling technology that is at the basis of all orbit determination, state estimation, guidance, navigation and control, impact and collision prediction processes. In particular, in the case of space debris orbit analysis, uncertainty propagation is required to predict possible collisions or to describe the evolution of a cloud of particles. The latter, in fact, can be seen as the evolution of an uncertainty region over which one can define a distribution function. The evolution of an uncertainty region can be described through a linear model by multiplying the variation of the uncertain variables by the state transition matrix of the linearized dynamics. It can be shown that this approach is not suitable to correctly represent the evolution of an uncertainty region even over a short period of time. For this reason, in recent times, authors have proposed higher order methods either intrusive or non-intrusive. In the latter category one can find the work of Jones et al.[1] on the use of non-intrusive Polynomial Chaos Expansions to predict the collision of two objects or the work of Garmier et al.[2] and of De Mars et al.[3] on the use of Gaussian mixture models. Among the intrusive approaches one can find the work of Morselli et al.[4] on the use of Taylor models and the work of Park and Scheers[5] on the use of high order Taylor expansions. The approach proposed by Park and Scheeres has the main drawback

[*]PhD candidate, Department of Mechanical & Aerospace Engineering, University of Strathclyde, 75 Montrose Street, Glasgow, UK.

[†]Professor, Department of Mechanical & Aerospace Engineering, University of Strathclyde, 75 Montrose Street, Glasgow, UK.

[‡]Lecturer, Department of Mechanical & Aerospace Engineering, University of Strathclyde, 75 Montrose Street, Glasgow, UK.

[§]Research Fellow, Department of Mechanical & Aerospace Engineering, University of Strathclyde, 75 Montrose Street, Glasgow, UK.

that the construction of the polynomial representation of the uncertainty region of the end states requires the propagation of the partial derivatives of the Taylor expansion of the dynamics. As the dimension of the uncertain space and the order of the expansion increase, the number of required propagations grow faster than the number of coefficients of the Taylor expansion and becomes more expensive than a Monte Carlo sampling. The use of a dedicated algebra to manipulate the Taylor expansions reduces this problem as the operations are performed only on the required coefficients up to the desired order. Even in this case, however, the number of terms in the expansion grows as $(d+n)!/(d!n!)$ with n the number of dimensions and d the degree of the polynomial.

The main advantage of non-intrusive methods is in the ability to work with generic models, also in the form of black-boxes, and with little requirements on the coding of the models or on their regularity. This advantage is interesting when a set is propagated through a complex system model that cannot be expressed in a simple analytical form.

This paper will present an assessment of the accuracy and computational cost of four different non-intrusive approaches to propagate an uncertainty region in orbital mechanics, and to build a high order nonlinear representation of the quantity of interest. The approaches are: a Polynomial Chaos Expansion (PCE), an Uncertainty Quantification-High Dimensional Model Representation (UQ-HDMR) a Generalised Kriging model and an expansion with Tchebycheff polynomials on sparse grids. Unlike previous works in which the PCE was used to build a spectral representation of the distribution of the quantity of interest, in this paper we use each approach to build a model representation of the propagated uncertainty region. All the four approaches are compared to a Monte Carlo sampling on four different scenarios with objects orbiting around Earth in different regimes.

The paper is organized as follows. We start with a brief description of the four non-intrusive polynomial approaches. Then we present the test cases and the dynamical model used in the experiments. Finally, we show the results of the comparison.

NON-INTRUSIVE METHODS

Monte Carlo methods are the most popular methods in many mathematical and physical problems that may involve optimization, numerical integration and random sampling from a probability distribution. To construct the shape of the probability distribution of the output state variables of a dynamical system, a Monte Carlo method works in the following way:

1. Define the domain of the input variables (both state variables and dynamical parameters) of the dynamical systems.

2. Generate a random sample of the inputs according to their probability distribution.

3. Evaluate the dynamical system with initial condition on each random point to obtain the corresponding final state. This is a deterministic computation.

4. Estimate the expectation of the final state.

Although Monte Carlo methods use the dynamical model as a black-box and do not require any assumption on its regularity, drawing samples from their known probability distribution is a challenging problem, especially in high-dimensional spaces.

An alternative to Monte Carlo sampling is represented by the construction of a surrogate model. The development of the response of a dynamical system to parameter and model uncertainty can be captured by a degree d polynomial in n dimensions. Then the sampling can be done using the polynomial approximation, provided that the result of the surrogate model and the true values of the dynamics is accurate enough. This process is still of computational complexity of order of the number of samples but each computation is fast.

In this paper we compare four different polynomial approximations. The first uses Legendre polynomials and the polynomial basis contains all terms up to the maximum degree of expansion. The second uses Tchebycheff polynomials but discarded some terms of degree smaller than the maximum degree. The third one uses a mixture of kernel functions, e.g., Gaussian kernels, and treat the response as a combination of a deterministic and a stochastic process. Such a model is normally referred to as Generalized Kriging model. The last one uses high-dimensional model representation that allows for a reduction of the number of terms in the expansion combined with sparse grids.

Polynomial Chaos Expansion

Polynomial Chaos Expansion considers orthonormal polynomials as basis functions. Since we are assuming uniform random variables, Legendre polynomials are the used. A multidimensional basis of orthonormal polynomial is given by the product of unidimensional terms:

$$\mathcal{L}_\alpha(\mathbf{x}) = \prod_{i=1}^{d} L_{\alpha_i}(x_i)\,, \qquad \alpha = (\alpha_1, \ldots, \alpha_n)\,, \tag{1}$$

where n is the dimension of $\mathbf{x}$ and α is a multi-index array.

We want to find the linear combination of multivariate Legendre polynomials of degree up to d in n variables such that:

$$\hat{X}(\mathbf{x}) = \sum_{\alpha \in \Delta_{d,n}} c_\alpha \mathcal{L}_\alpha(\mathbf{x})\,, \tag{2}$$

where, in our case, X is the response of the dynamical system, $\mathbf{x}$ a random sampling from the distribution of the initial uncertainty variables, c_α are the unknown coefficients to be determined, and

$$\Delta_{d,n} = \{\alpha \in \mathbb{N}^n : |\alpha| \leq d\}\,,$$

with $|\alpha| = \alpha_1 + \ldots + \alpha_n$.

The unknown coefficients can be found by least square method on sample points. We choose samples random from a hypercube and at least equal in number to the number of terms in the multivariate basis, that is $(d+n)!/d!n!$, the cardinality of $\Delta_{d,n}$. This approach is traditionally referred as the Total Order Expansion. Although this number is far lower than the one required for a full Monte Carlo analysis, the number of samples still grows significantly with the number of dimensions.

We can summarized the PCE approximation as follows:

1. Define the domain of the input variables (both state variables and dynamical parameters) of the dynamical systems as hypercube.
2. The Legendre basis consists of all the polynomials with degree less or equal than d in n variables.

3. Select M random sample points from the domain.

4. Evaluate the dynamical system with initial conditions the M points.

5. Compute the unknown coefficients such that the error between the true response and its approximation is minimized at the sample points.

High Dimensional Model Representation

A major drawback of using non-intrusive uncertain quantification (UQ) methods is the curse of dimensionality, that is the number of samples grows exponential with the number of uncertain variables. This limits the usage of non-intrusive techniques to a low number of random variables, i.e. less than five. The High Dimensional Model Representation (HDMR) can handle the curse of dimensionality by decoupling the stochastic space into sub-domains and interpolate only the low order sub-domains. Each sub-domain is sampled with a different number of samples, which allows to use the optimal number of samples for each sub-domain, thus reducing the number of function evaluations. Moreover, it is also interpolated with an independent technique and the final model is then constructed as sum of these models. However, this approach requires a special sampling strategy, so random sampling cannot be used. A simplified UQ-HDMR scheme is the following:

1. Sample the first order increment functions

$$dF_i(x_i) = \int_{x_i^c}^{x_i} \frac{\partial F(x^*)}{\partial \xi_i} d\xi_i = F(x^*) - F(x^c)\,, \qquad i = 1, \ldots, n$$

   where n is the number of variables, x_i^c is the anchor point in the i-variable needed to start the ANOVA expansion, $x^* = ({}^c x_1, \ldots, x_i, \cdots, {}^c x_n)$ and ${}^c x = ({}^c x_1, \ldots, {}^c x_n)$.

2. Select the maximum order of interactions, e.g. 2 or 3. In many works, it was proven that low order interactions well describe the problem of interest and in Kubicek et al.[6] is explained why this phenomena is happening. In this work, the maximum order is restricted to 3.

3. Sample the higher order interactions according to the following equation:

$$N = n_j^{-1/k} d^{-k}\,,$$

   where n_j is the number of samples in one-dimension quadrature in the given direction, d is the order of increment function and k is the coefficient growth, which is prescribed by user. The N represents the number of samples in given direction for given order of increment function. The position of the new samples is given by a position of samples from the lower domains.

4. Create the surrogate model of the given increment function, e.g. using a Lagrange interpolation with the 1-D Clenshaw-Curtis sampling strategy.

It is well known that the HDMR accuracy is sensitive to the selection of the central point (see Zhongqiang et al.[7]). Various methods have been proposed to overcome this problem. However, all these methods require a pre-sampling strategy approach, which leads to unaffordable computational burden. On the other hand, if all increment functions are included in the final model, the influence of the central point completely disappear. Therefore, if all important increment functions are selected,

the influence of the central point diminish and this leads to an accurate model regardless of the central point. The central point is selected as a mean value of the input distribution.

For a detailed explanation of the method see Kubicek and Minisci[8] where the tested approach has been compared to PCE and Monte Carlo sampling on three benchmark problems.

In this paper, two approaches are tested. The first approach represents the isotropic grow in number, where all the random variables are treated equally. The second one is the anisotropic approach. This approach allows to use various number of samples for each direction and thus obtain the best accuracy for a low number of samples.

Generalized Kriging

Kriging is a commonly used method of interpolation (prediction) for spatial data. The data are a set of observations of some variables of interest, with some spatial correlation present. Usually, the result of Kriging is the expected value and variance computed for every point within a region.

Interpolation with Kriging has some advantages. It compensates for the effects of data clustering by assigning to individual points within a cluster less weight points. It also gives the estimate of the error (kriging variance), along with the estimate of the variable itself. Moreover, it can improve the accuracy locally. Its major drawback is the need of a fine enough grid, especially in high dimensonality.

There are many variants of Kriging estimators. However, all of them can be considered mixture of Gaussian process. In our comparison we use the open source Matlab toolbox DACE[9] to create the Kriging surrogate with Gaussian correlation and a polynomial regression of order 2 as regression model.

Tchebycheff polynomial approximation

Univariate Tchebycheff polynomials are an orthogonal basis over the space $\mathcal{C}^{\infty}[-1,1]$ and the truncate Tchebycheff series are close to the best uniform polynomial approximation for a given continuous function.[10,11]

The approximation algorithm with Tchebycheff series works as the PCE by substituting multivariate Legendre polynomial basis with multivariate Tchebycheff polynomial basis. The curse of dimensionality in high dimensional uncertainty space is tackled by choosing points on a sparse grid.

The most popular sampling methods use Smolyak sparse grids,[12] where the number of samples grows polynomially with the degree d, instead of exponentially. The number of elements to be included is controlled by a parameter μ, called level of approximation, which has the same role as the order of expansion in the Taylor series. In this work sparse grids are generated using extrema of unidimensional Tchebycheff polynomials as described in Judd et al.[13]

The reduced number of points allow also to reduce the number of terms in the Tchebycheff polynomial basis, and so the number of unknown coefficients. The basis functions are chosen from all the polynomials up to degree d in n variables according to the level of approximation. They tend to exclude cross products terms under the assumption that higher order correlations are generically negligible.

Using the same notation as in the PCE section, we want to find the linear combination of multivariate Tchebycheff polynomials of level of approximation μ (and maximum degree 2^{μ}) in n

variables:

$$\hat{X}(\mathbf{x}) = \sum_{\alpha \in \mathcal{H}^{n,\mu}} c_\alpha \mathcal{T}_\alpha(\mathbf{x}) \,, \tag{3}$$

where

$$\mathcal{H}^{n,\mu} = \{\alpha \in \mathbb{N}^n : \alpha \text{ satisfies the Smolyak rule at level } \mu\} \,.$$

The unknown coefficients are computed via a Lagrange interpolation at the Tchebycheff nodes given by the sparse grid of level μ. For more details see Riccardi et al.[14]

NUMERICAL EXPERIMENTS

We propose four different scenarios to compare the non-intrusive methods described in the previous section to a standard Monte Carlo sampling:

1. Low-Earth orbit with 6 uncertain parameters (LEO6): the components of position and velocity at the initial states.
2. Low-Earth orbit with 10 uncertain parameters (LEO10): the components of position and velocity at the initial states, plus two uncertain model parameters.
3. Highly elliptical orbit with 6 uncertain parameters (HEO6): the components of position and velocity at the initial states.
4. Highly elliptical orbit with 10 uncertain parameters (HEO10): the components of position and velocity at the initial states, plus two uncertain model parameters.

The computational cost is measured using the number of sample points.

Dynamical model

To compare the approximation provided by the four methods we use a dynamical model containing the main perturbations acting on a satellite of negligible mass orbiting in low-Earth orbit. The main gravitational perturbation is due to the non-spherical shape of the Earth: the most relevant effect is due to the J_2 coefficient in the development of the Earth's potential in spherical harmonics. Among the non-gravitational perturbations there are the solar radiation pressure (SRP) and the atmospheric drag.

In an equatorial reference frame, the dynamical equations can be written as

$$\begin{aligned} \dot{\mathbf{r}} &= \mathbf{v} \\ \dot{\mathbf{v}} &= \mathbf{F}_{J_2} + \mathbf{F}_{SRP} + \mathbf{F}_{drag} \,, \end{aligned} \tag{4}$$

where $\mathbf{r}, \mathbf{v}$ are the position and velocity vectors, $\mathbf{r}_0 = \mathbf{r}(t_0), \mathbf{v}_0 = \mathbf{v}(t_0)$ are the initial conditions at the initial time t_0, and (see, e.g., Milani et al.,[15] Sharaf and Selim[16])

$$\mathbf{F}_{J_2} = -\frac{\mu}{r^3} r + 3\,\frac{\mu J_2 R_e^2}{2}\,\frac{\mathbf{r}}{r^5}\left(\mathbf{r} + 2\,z - \frac{5z^2}{r^2}\right), \tag{5}$$

$$\mathbf{F}_{SRP} = \frac{\phi_\odot}{c}\,C_R\,\frac{A}{m}\,\hat{\mathbf{S}}\,, \tag{6}$$

$$\mathbf{F}_{drag} = -\frac{1}{2}\,C_D\,\frac{A}{m}\,\rho\,v^2\hat{\mathbf{v}}\,, \tag{7}$$

where μ is the gravitational parameter, R_e is the mean Earth's equatorial radius, (x, y, z) and r are, respectively, the components and the modulus of $\mathbf{r}$, $\phi_\odot$ is the solar radiation flux, c is the velocity of light, C_R is the reflectivity coefficient, A/m is the area-to-mass ratio, $\hat{\mathbf{S}}$ is the direction of the Sun, C_D is the drag coefficient, and ρ is the density of the air atmosphere given by the NRLSISE-00 athmospheric model.[17]

Uncertainty space

The uncertainty space is assumed to be a hypercube. The PCE-Legendre and Kriging use a random sampling from a latin hypercube, the Tchebycheff and UQ-HDMR use sparse grids with Clenshaw-Curtis points. However, UQ-HDMR uses various numbers of samples for each order and direction thus leading to a low number of samples for a high accuracy.

The uncertainty variables are the components of the position and velocity vectors $\mathbf{r}, \mathbf{v}$ and/or four dynamical parameters $A/m, C_R, C_D$ and $F_{10.7}$. The last one represents the daily solar flux for previous days, and it is varied here to model the uncertainty on the air density. The bounds for the dynamical parameters are reported in Table 1.

Table 1: Uncertainty bounds for the dynamical parameters.

	A/m	C_R	C_D	$F_{10.7}$
Lower bound	0.001	1.0	1.5	100
Upper bound	0.1	2.0	3.0	200

As initial conditions for the state vector, a LEO and HEO orbit have been chosen from the TLE orbit catalog available from the space-track website.[18] The values are reported in Table 2. The uncertainty bounds are set in the Cartesian coordinate space and are assumed to be $10^{-5} \cdot r_0$ and $10^{-5} \cdot v_0$, where r_0 and v_0 are the magnitude of the initial position and velocity vector expressed in km and km/s, respectively.

Table 2: Keplerian orbital elements of the LEO and HEO orbit as of May 26, 2015.

ID	a [km]	e	i [deg]	Ω [deg]	ω [deg]	ℓ [deg]
40650	7006.96	0.0008315	98.1533	165.9974	100.2845	259.5405
40618	24204.56	0.7278988	25.4766	31.5897	179.4183	182.5857

The propagation time span is set to $40\,P$, where P is the period of the unperturbed orbit. It is to about 4 days for the LEO orbit and 60 days for the HEO orbit. All simulations have been implemented in MATLAB and run on an Intel i7 3.40 GHz.

Experimental set up

The approximated polynomial computed by each of the four non-intrusive method is evaluated in $M = 1\,000 \times n$ points, where n is the number of uncertainty variables. The points are distributed according to the Latin Hypercube sampling approach. The result is then compared with the true state given by the forward propagation through the dynamics of the Monte Carlo points. The estimation

of the error between the approximation $\hat{X}$ and the true value X is given by the root mean square error

$$\mathrm{RMSE} = \sqrt{\frac{1}{M}\sum_{i=1}^{M}(\hat{X}_j(\mathbf{x}_i) - X_j(\mathbf{x}_i))^2}\,, \qquad j = 1, \ldots, 6\,, \tag{8}$$

where $\mathbf{x}_i$ represents a single Monte Carlo point vector.

Figure 1 shows the uncertainty regions in the 3D space for each scenarios. The effect of the dynamical parameters is to enlarge the uncertainty region for the LEO orbit and stretch it along the trajectory for the HEO. As result, the dependence of the final state with respect to the initial conditions is highly non-linear.

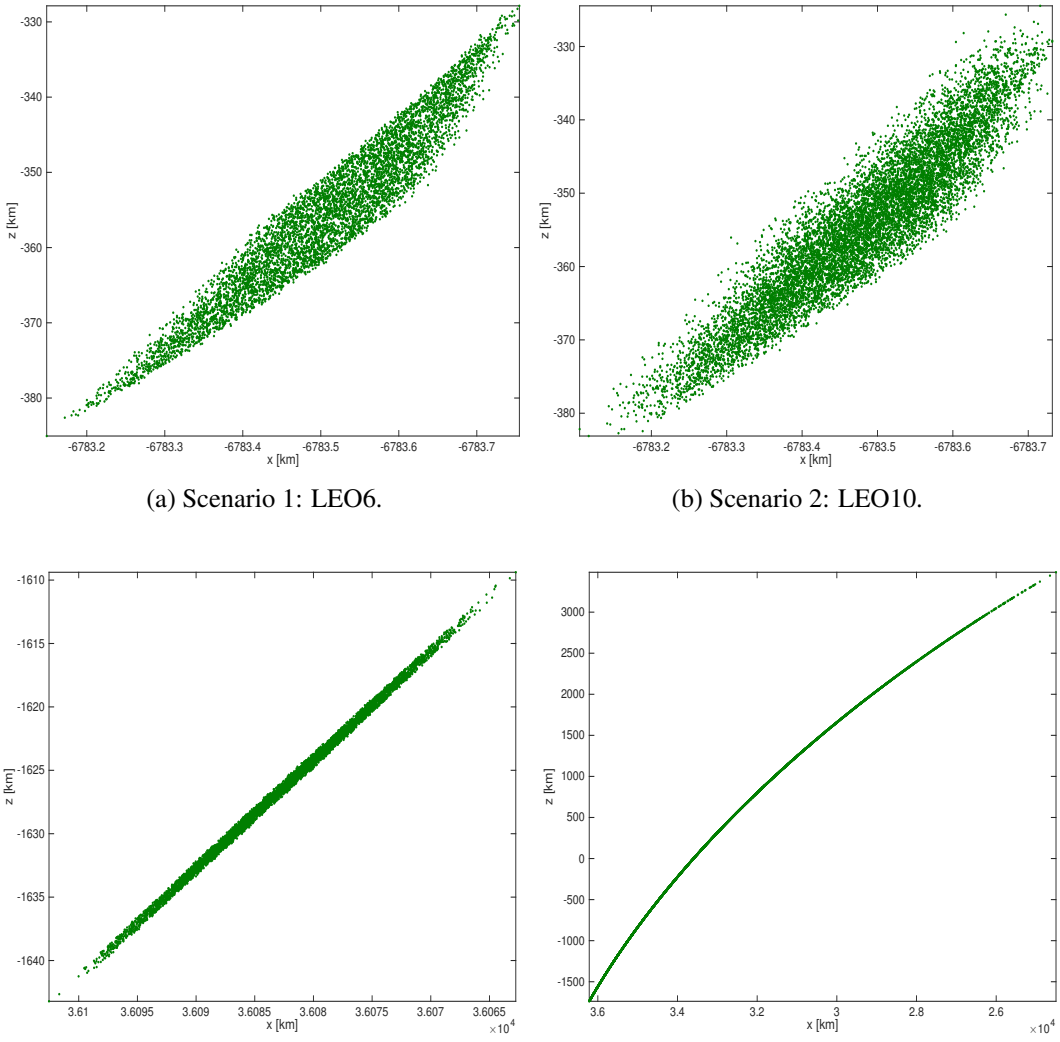

(a) Scenario 1: LEO6.

(b) Scenario 2: LEO10.

(c) Scenario 3: HEO6.

(d) Scenario 4: HEO10.

Figure 1: Uncertainty region of the final state.

The convergence of the polynomial approximation is presented in Figure 3, Figure 4, Figure 5 and Figure 6. The estimation of the accuracy is given by the RMSE of each component of the final

state $x_1, \ldots, x_6$ with respect to the Monte Carlo outcomes as a function of the number of sample points used to build the polynomial approximation. We use the same legend for all figures, that is reported in Figure 2.

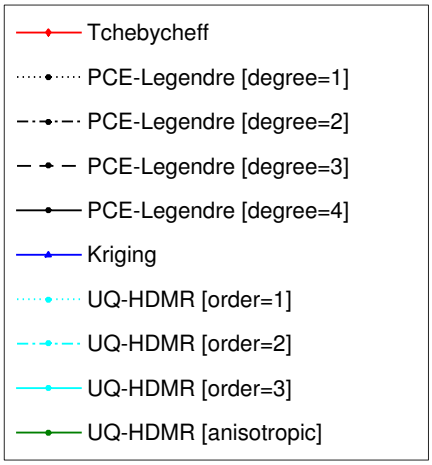

Figure 2: Legend of the Figures 3, 4, 5 and 6.

In all the examples, Kriging exhibits the slowest convergence, meaning that for a fixed number of sample points it has the highest value for the RMSE.

The uncertainty region of scenario 1 (LEO6) can be approximated with less than 100 sample points and a maximum RMSE of 10^{-5} km by all methods with the exception of Kriging. The best accuracy is reached with a PCE-Legendre of degree 3. Tchebycheff and UQ-HDMR anisotropic show equal behavior. (Figure 3). However, the UQ-HDMR approach exhibits bigger flexibility in terms on number of samples over the Tchebycheff.

By adding the uncertainties on four dynamical parameters (scenario 2), the dependencies become highly non-linear and to obtain an accuracy of order 10^{-3} km a PCE-Legendre of degree less or equal than 4 or a Tchebycheff sparse basis of level less or equal 3 needs to be used (see Figure 4).

The results for scenario 3 (HEO6) are shown in Figure 5. A PCE-Legendre of degree 1 dominates higher order PCE-Legendre and all the Tchebycheff approximations and Kriging. However, the best approximation is given by the UQ-HDMR, both for the isotropic and anisotropic approach. Moreover, the UQ-HDMR performs the best in terms of sampling.

Figure 6 presents the analysis for scenario 4 (HEO10). As for scenario 2, the dependencies are highly non-linear. Tchebycheff and UQ-HDMR with the anisotropic approach show comparable results. Again, the UQ-HDMR is slightly better and more flexible over the Tchebycheff in terms of sampling.

Finally, for each test case we fixed the accuracy σ and we find the minimum number of sample points such that $\max(\mathrm{RMSE}) < \sigma$, where the maximum is taken over the components of the final state vector (see Tables 3, 4, 5 and 6). The values of UQ-HDMR correspond to the anisotropic approach. The accuracy has been fixed to $4D \cdot 10^{-4}$, where D is the diameter of the projection of the uncertainty region of the final state on the (x, z)-plane.

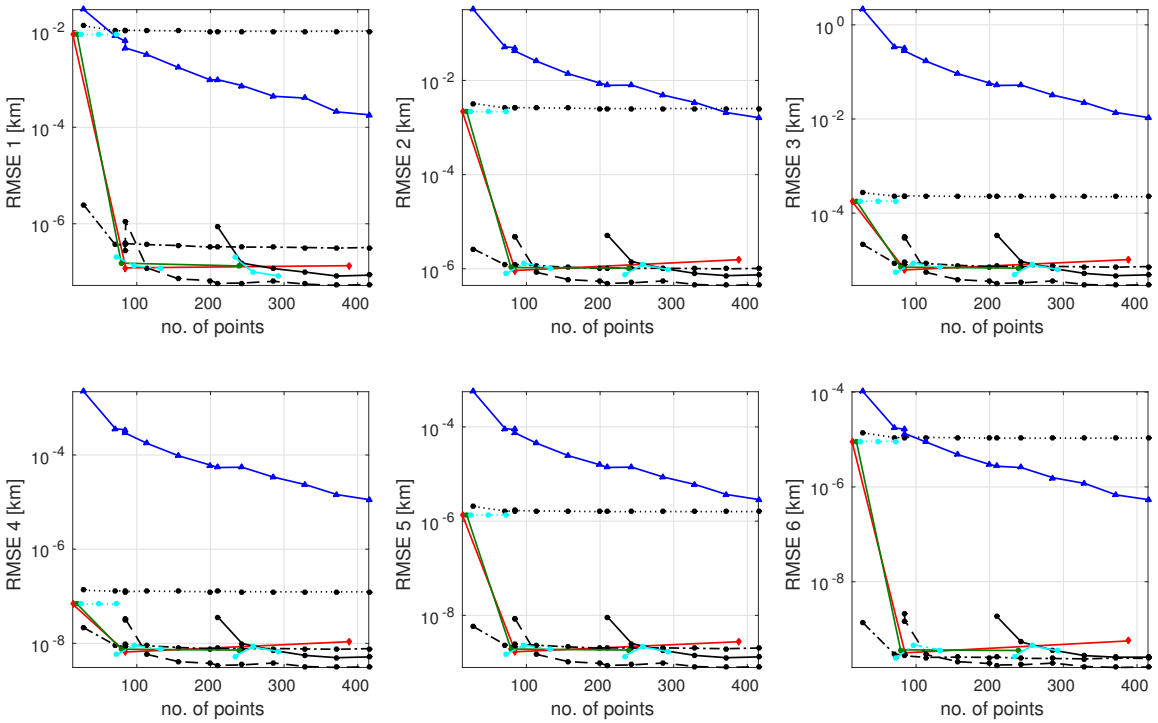

Figure 3: The RMSE as a function of the number of the sample points for scenario 1 using 6 000 Monte Carlo points.

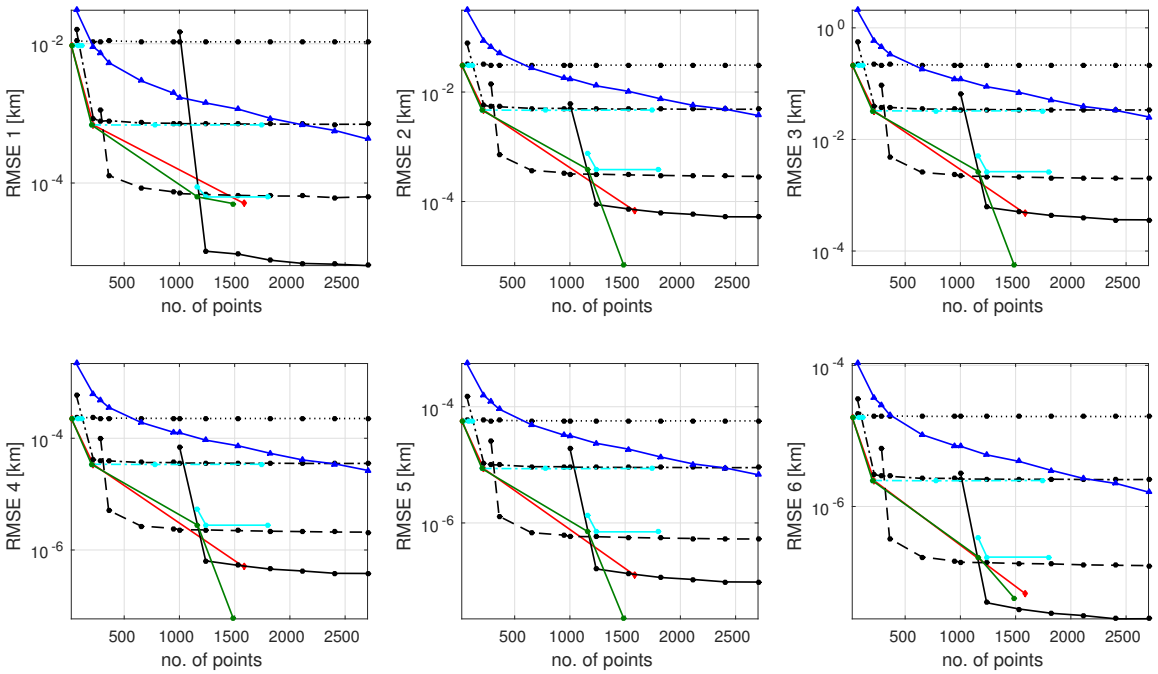

Figure 4: The same as Figure 3 applied to scenario 2 with 10 000 Monte Carlo test points.

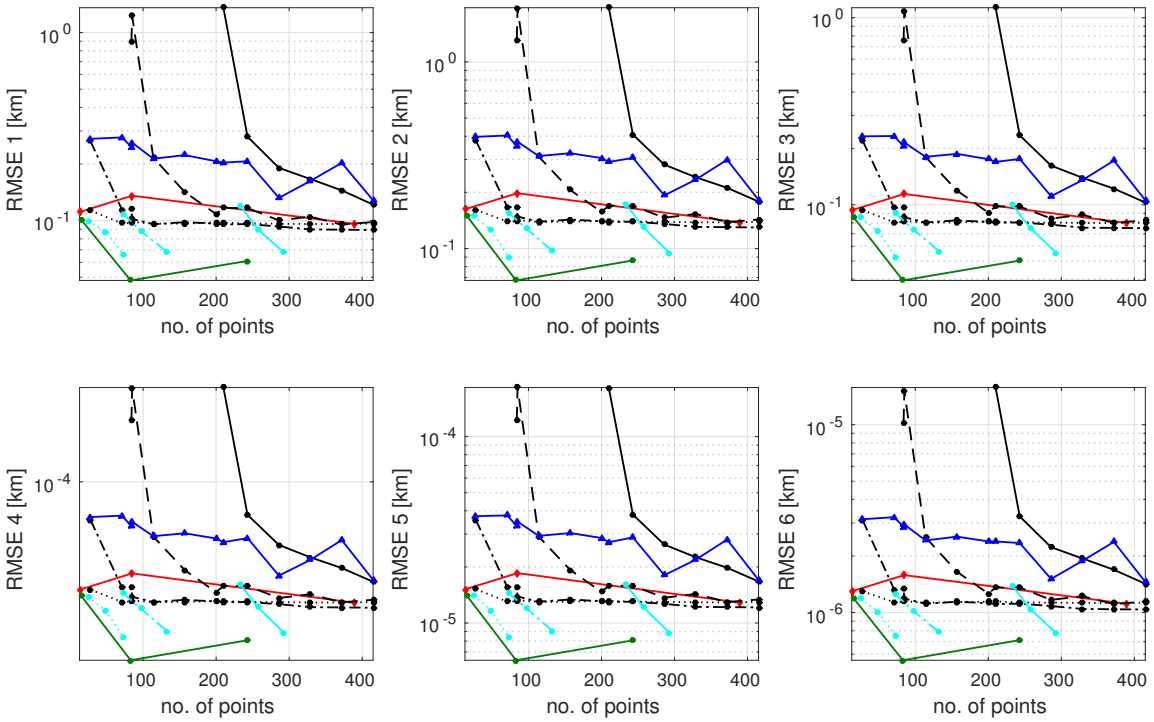

Figure 5: The same as Figure 3 applied to the HEO orbit in scenario 3 with 6 000 Monte Carlo points.

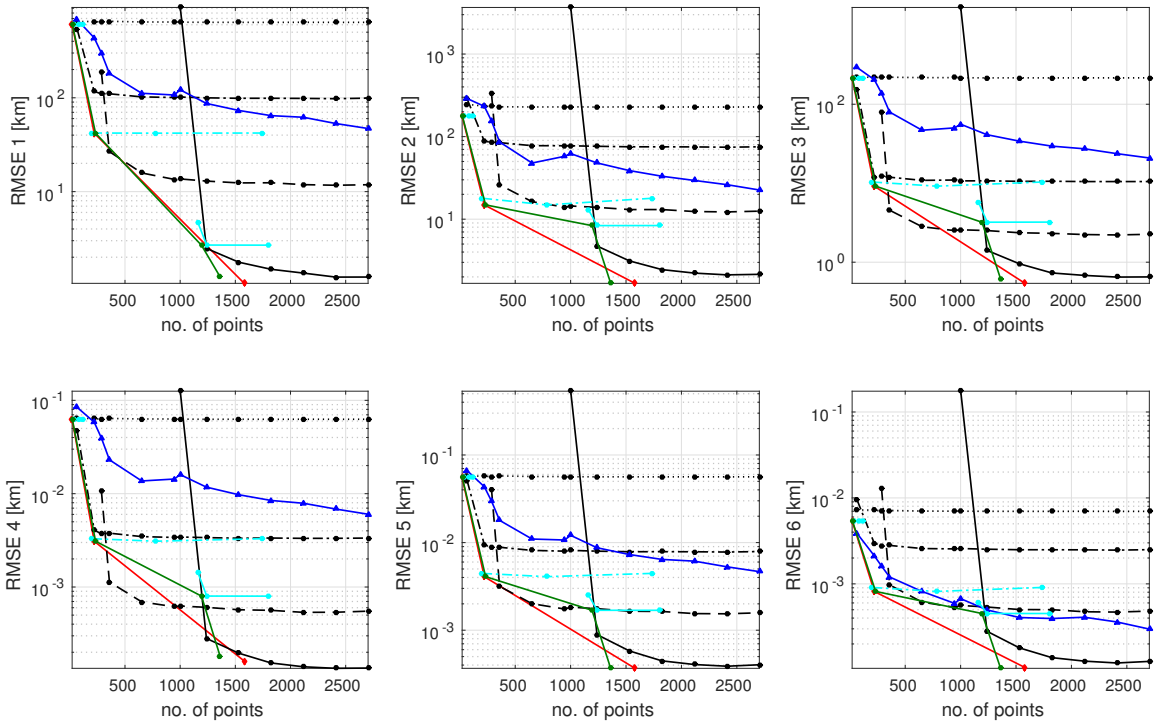

Figure 6: The same as Figure 4 applied to the HEO orbit in scenario 4 with 10 000 Monte Carlo points.

Table 3: Summary of the comparison for scenario 1 with a reference accuracy of 0.229 km.

Method	No. of sample points	$\max(\mathrm{RMSE})$
Tchebycheff	13	0.00833
PCE-Legendre	28	0.01262
UQ-HDMR	19	0.00833
Kriging	144	0.16753

Table 4: Summary of the comparison for scenario 2 with a reference accuracy of 0.235 km.

Method	No. of sample points	$\max(\mathrm{RMSE})$
Tchebycheff	21	0.21433
PCE-Legendre	66	0.22553
UQ-HDMR	23	0.21437
Kriging	652	0.18307

Table 5: Summary of the comparison for scenario 3 with a reference accuracy of 0.209 km.

Method	No. of sample points	$\max(\mathrm{RMSE})$
Tchebycheff	13	0.16224
PCE-Legendre	28	0.16147
UQ-HDMR	15	0.15068
Kriging	286	0.19265

Table 6: Summary of the comparison for scenario 4 with a reference accuracy of 51.317 km.

Method	No. of sample points	$\max(\mathrm{RMSE})$
Tchebycheff	221	41.970
PCE-Legendre	359	26.658
UQ-HDMR	233	41.976
Kriging	2703	41.044

CONCLUSIONS

We compare four different non-intrusive approaches applied to the propagation of uncertainty in orbital dynamics under different orbit regime and uncertainty both on the orbital parameters and dynamical models. If only the uncertainties on the orbital elements are taken into account, a low order polynomial of degree at most 2 is enough to represent the uncertainty region of the final states as a function of the initial uncertain parameters. When also the uncertainty on the dynamical parameters are considered, the region becomes highly non linear and higher order polynomials are needed. In order to reduce the number of sample points in high dimensional problem, sparse grids and Tchebycheff polynomial expansions were shown to give reliable results at a reduced computational cost. In this sense the use of PCE-Legendre gave mixed results. On the other hand the use of sparse grids and sparsity promoting techniques like compressive sampling are expected to reduce the computational cost.

UQ-HDMR provided comparatively good results on all test functions at a computational cost comparable to the Tchebycheff approximation on sparse grids. In scenario 3, it is the most afforadable and accurate technique of all four. In scenraio 2, the anisotropic case is able to achieve the best accuracy in 4 tested cases. In scenario 4, it achieve the same accuracy as the PCE and the Tchebysheff, yet for a lower number of samples.

The generalized Kriging was shown to require a high number of sample points and to provide the worst approximation of the final states. Note that the hyperparameters were optimized in all cases to maximize the likelihood. Different correlation and regression functions are indeed possible and might improve the performance of the Kriging approximation. Note that the Kriging approximation allows adding sample points where the estimated variance is high without following any particular pattern. This feature is of considerable importance when the surrogate is used within an optimization process. In this sense the other methods, using a structured grid, need a dedicated treatment if a local improvement is required.

ACKNOWLEDGMENT

The work in this paper was partially supported by the Marie Curie FP7-PEOPLE-2012-ITN Stardust, grant agreement 317185.

REFERENCES

[1] B. A. Jones, A. Doostan, and G. H. Born, "Nonlinear Propagation of Orbit Uncertainty Using Non-Intrusive Polynomial Chaos," *Journal of Guidance Control Dynamics*, Vol. 36, mar 2013, pp. 430–444, 10.2514/1.57599.

[2] R. Garmier, B. Revelin, P. Legendre, S. Delavault, B. Vidal, and L. Lorda, "Computation of a Collision Probability Based on a Gaussian Mixture Model of the TLE Accuracy," *ISSFD2009, September 28 - October 2, Toulouse, France*, 2009.

[3] K. J. De Mars and M. K. Jah, "Probabilistic Initial Orbit Determination Using Gaussian Mixture Models," *Journal of Guidance, Control, and Dynamics*, Vol. 36, No. 5, 2013, pp. 1324–1335.

[4] A. Morselli, R. Armellin, P. Di Lizia, and F. Bernelli-Zazzera, "A High Order Method for Conjunctions Analysis: Monte Carlo Collision Probability Computation," *Advances in Space Research*, Vol. 55, No. 1, 2015, pp. 311–333.

[5] R. S. Park and D. J. Scheeres, "Nonlinear Mapping of Gaussian Statistics: Theory and Applications to Spacecraft Trajectory Design," *Journal of Guidance, Control, and Dynamics*, Vol. 29, No. 6, 2006.

[6] M. Kubicek, E. Minisci, and M. Cisternino, "High dimensional sensitivity analysis using surrogate modeling and High Dimensional Model Representation," *International Journal of Uncertainty Quantification*, 2015. accepted.

[7] Z. Zhongqiang, M. Choi, and E. G. Karniadakis, "Anchor points matter in ANOVA decomposition," *Spectral and High Order Methods for Partial Differential Equations. Springer Berlin Heidelberg*, 2011, pp. 347–355.

[8] M. Kubicek and E. Minisci, "High dimensional uncertainty quantification using the derivative approach," *11th World Congress on Computational Mechanics (WCCM XI, ECCM V, ECFD VI), Barcelona, Spain, September 2014*.

[9] "DACE: A Matlab Kriging Toolbox.," `http://www.imm.dtu.dk/~hbn/dace/`.

[10] J. C. Mason, "Near-best multivariate approximation by Fourier series, Tchebycheff series and Tchebycheff interpolation," *Journal of Approximation Theory*, Vol. 28, No. 4, 1980, pp. 349–358.

[11] B. Franklin, *Chebyshev Expansions*. 2007.

[12] S. Smolyak, "Quadrature and interpolation formulas for tensor products of certain classes of functions," *Dofl. Akad. Nauk*, Vol. 158, 1963, pp. 1042–1045.

[13] K. L. Judd, L. Maliar, S. Maliar, and R. Valero, "Smolyak method for solving dynamic economic models: Lagrange interpolation, anisotropic grid and adaptive domain," *Journal of Economic Dynamics and Control*, Vol. 44, No. 1-2, 2014, pp. 92–123.

[14] A. Riccardi, C. Tardioli, and M. Vasile, "An intrusive approach to uncertainty propagation in orbital mechanics based on Tchebycheff polynomial algebra," *AAS Astrodynamics Specialists Conference, Vail, Colorado, USA, August 9–13*, 2015. AAS 15-544.

[15] A. Milani, A. Nobili, and P. Farinella, *Non-gravitational perturbations and satellite geodesy*. Adam Hilger, Bristol, 1987.

[16] M. A. Sharaf and H. H. Selim, "Final state predictions for $J-2$ gravity perturbed motion of the Earth's artificial satellites using Bispherical coordinates," *NRIAG Journal of Astronomy and Geophysics*, Vol. 2, No. 1, 2014, pp. 134–138.

[17] J. M. Picone, A. Hedin, D. P. Drob, and A. C. Aikin, "NRLMSISE-00 empirical model of the atmosphere: Statistical comparisons and scientific issues," *J. Geophys. Res.*, Vol. 107, No. A12, 2002, p. 1468.

[18] "Space-track website," `https://www.space-track.org`.